

Pyrochlore supergroup minerals from the alkaline pegmatites in the Larvik Plutonic Complex, southern Norway

Paula C. Piilonen, Glenn Poirier, Ralph Rowe & Alf Olav Larsen

Introduction

Pyrochlore supergroup minerals are ubiquitous phases within all alkaline pegmatites in the Larvik Plutonic Complex, Oslo rift, southern Norway. It was first discovered in the 1820's by N.O. Tank from a locality near Stavern, Larvik, Vestfold, and was described in 1826 by Wöhler. Pyrochlore was the second mineral to be described as a new species from the alkaline pegmatites of the Larvik Plutonic Complex, next to zirconolite (*polymignite*). It is one of the earliest minerals to crystallize in the alkaline pegmatites, and occurs dominantly as subhedral to anhedral yellow, orange and reddish-orange to dark red-brown grains up to 1 cm in width embedded in perthitic feldspar, amphibole, aegirine, magnetite and zircon. Primary, euhedral octahedra up to 2-4 cm have been found at Stavern (Larvik, Vestfold; Fig. 1) and Stokkøya (Langesundsfjord). The majority of these pyrochlore supergroup minerals are metamict and have undergone extensive alteration. Late-stage euhedral crystals of pyrochlore, most only a few mm's across, are often late-stage phases, found crystallizing on acicular aegirine in the agpaitic pegmatites at Lysebo (Hedrum). Pyrochlore supergroup minerals have only rarely been found in the agpaitic pegmatites in ring sections 9 and 10; perovskite-group minerals are the common Nb-oxide phase.



Fig. 1. Pyrochlore crystal from the Håkestad quarry, Tjølling, Larvik, collected in June 2000. The crystal is 10 mm along the edge. Collection and photo A.O. Larsen.

In an effort to shed light on the geological, geochemical and mineralogical processes that have collectively contributed to the formation and evolution of the alkaline pegmatites of the Larvik Plutonic Complex, a series of studies have been undertaken on the rock-forming and important accessory minerals. Being a primary, ubiquitous magmatic phase, pyrochlore supergroup minerals allow us to determine the high field-strength element characteristics of the magma from which the pegmatite formed. In addition, the susceptibility of pyrochlore supergroup minerals to post-magmatic and post-metamictization alteration by fluids allows for determination of the composition of the hydrothermal and meteoritic fluids which infiltrated the pegmatites following crystallization.

Primary pyrochlore supergroup minerals were sampled from 26 alkaline pegmatites across the Larvik Plutonic Complex (Table 1, Fig. 2) in order to determine their chemical composition and examine their alteration patterns. Species names were applied to each specimen in accordance with the new pyrochlore supergroup nomenclature proposed by the IMA (Atencio et al. 2010).

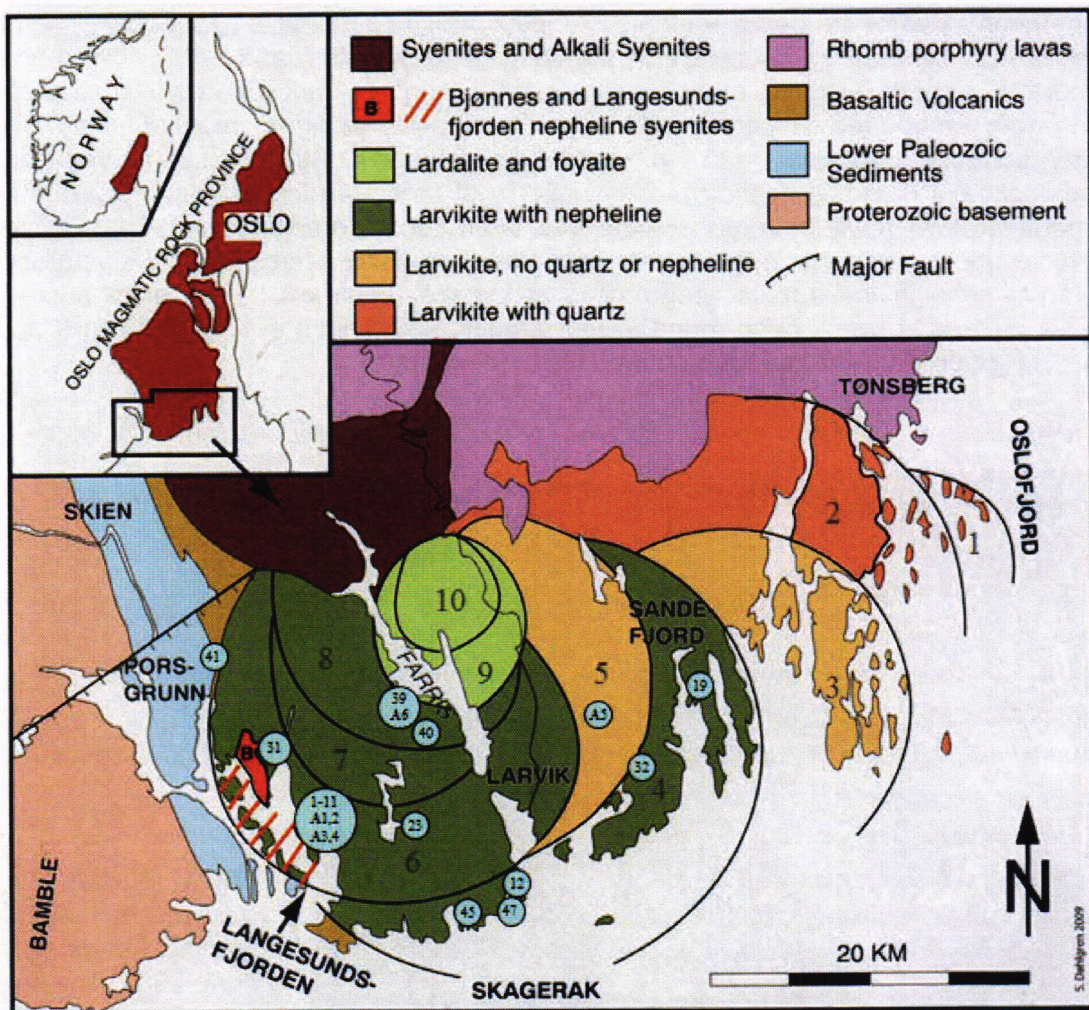


Fig. 2. The Larvik Plutonic Complex (LPC) showing the 10 ring sections (RS) and pyrochlore supergroup sample locations. The oldest RS occur in the east and are miaskitic. Younger plutons have intruded successively westward, becoming increasingly peralkaline. From Dahlgren (2010), modified from Petersen (1978).

Chemical composition

Chemical analyses of pyrochlore supergroup minerals were done with a JEOL Superprobe 8230 at the University of Ottawa. Operating conditions were as follows: beam diameter of 5 μm , operating voltage 40 kV, and a beam current of 11 nA. A total of 29 elements were sought and the following standards and X-ray lines were employed: synthetic diopside (Si K α , Mg K α , Ca K α), sanidine (K K α , Al K α), rutile (Ti K α), VP₂O₇ (V K α), synthetic CePO₄ (Ce L α), Mn-columbite (Nb L α , Mn K α), synthetic LaPO₄ (La L α), synthetic NdPO₄ (Nd L α), synthetic SmPO₄ (Sm L α), synthetic PrPO₄ (Pr L α), synthetic YIG garnet (Y L α), zircon (Zr L α), hematite (Fe K α), celestine (Sr L β , S K α), microlite (F K α , Na K α), cassiterite (Sn L α), synthetic NiTa₂O₆ (Ta M α), synthetic UO₂ (U M α), synthetic ThO₂ (Th M α), galena (Pb M β), hafnon (Hf M α), apatite (P K α), and synthetic CoWO₄ (W M α). Count times for all elements except F were 20 seconds on peak, and 10 seconds on background. Count times for F were 50 seconds on peak and 25 seconds on background. Raw intensities were corrected using the PAP routine (Pouchou & Pichoir 1984). Table 2 contains EMPA data for pyrochlore supergroup minerals with formulae calculated on the anhydrous basis of two [6]^B-site cations (Nb+Ta,+Zr+ Hf+Ti+Fe³⁺+Sn+W+Si+Al = 2 apfu) in accordance with the Atencio et al. (2010).

Powder X-ray diffraction

Powder X-ray diffraction data for each pyrochlore supergroup sample were acquired at the Canadian Museum of Nature X-ray Diffraction Laboratory using a Bruker AXS D8 Discover equipped with a Hi-Star 2D detector and operated with a GADDS system. The instrument was calibrated using the statistical approach described by Rowe (2009). Analyses were performed at 40kV and 40mA with CuK α radiation and a sample-to-detector distance of 12 cm. All samples analysed are metamict and give only broad, potato-like peaks.

The pyrochlore supergroup

The pyrochlore supergroup displays an extraordinarily wide geochemical variability, including extensive non-stoichiometry. Pyrochlore supergroup minerals are cubic oxides ($Fd\bar{3}m$) with $a \sim 10.4 \text{ \AA}$ and $Z = 8$ (Rouse et al. 1998). They have a general formula $A_{2-m}B_2X_{6-w}Y_{1-n}$, where A = large [8]-coordinated cations (Na, Ca, Sr, Pb, Y, REE, U, Th), vacancies (\square) or H₂O, B = [6]-coordinated high field-strength (HFSE) cations (Nb, Ti, Ta, Sb, W), X = O, OH or F, and Y = OH, F, O, H₂O, \square , K, Cs or Rb. The symbols m , w and n represent incomplete occupancies in the A, X and Y sites, respectively. Values of m range from 0 to 2, $w = 0 - 0.7$ and $n = 0 - 1$ (Atencio et al. 2010). Calculation of a chemical formula is done on the basis of 2 B cations pfu (Nb+Ta,+Zr+ Hf+Ti+Fe³⁺+Sn+W+Si+Al = 2 apfu) as HFSE have been shown to be immobile during the alteration process and vacancies have not been found to occur in this site. The presence of high concentrations of SiO₂ (~ 10 wt.%) in altered pyrochlore supergroup mineral chemical analyses has been noted by many authors (Johan & Johan 1977; Uher et al. 1998; Chakhmouradian & Mitchell 2002; Bonazzi et al. 2006) and the role of Si in the structure, whether in the [6]-coordinated site, dispersed as an amorphous phase, or within metamictized regions, has been debated extensively by various authors. In LPC pyrochlore supergroup samples, Si has been included in the B site total but recognized that it is a result of post-metamictization alteration by late-stage, Si-bearing fluids and has not been used to name the species.

Five groups are recognized under the new nomenclature based on the dominant cation at the B site: pyrochlore (*sensu stricto*, Nb-dominant), betafite (Ti-dominant), microlite (Ta-dominant), roméite (Sb-dominant) and elsmoreite (W-dominant). These root names are further modified using the dominant species of the dominant valence at the Y site, and the dominant species of the dominant valence group at the A site (Atenico et al. 2010). For example, fluornatropyrochlore is the name for a pyrochlore group species which is F- and Na-dominant. Only 7 species are officially IMA-approved, whereas 20 additional species in the literature require complete descriptions in order to achieve valid species status (Atenico et al. 2010).

Alteration textures

Back-scattered electron images (BSEI) of all the samples reveal a wide range of alteration patterns. The majority of primary magmatic features have been overprinted by either primary or secondary alteration as defined by Lumpkin & Ewing (1995). Five main types of alteration are evident.

1. Unaltered grains with minimal penetrating, fracture-controlled alteration characterized by lower average Z (atomic number; e.g. LACP-23, Fig. 3A). A unique feature in these samples is the presence of fission tracks adjacent to altered fractures (Fig. 3B). Using terminology defined by Lumpkin & Ewing (1995), fracture-controlled alteration can be considered secondary alteration. It is possible that in many cases, the apparently “unaltered” grain has actually experienced primary alteration, with the required large-scale intracrystalline diffusion or coupled dissolution-reprecipitation having reached completion and the original composition no longer detectable.
2. Complex, diffuse-zoned grains with penetrating, fracture-controlled secondary alteration (Lumpkin & Ewing 1995) characterized by lower average Z (e.g. LACP-01, Fig. 3C). Such grains may contain both primary compositions and compositions which have undergone primary alteration. Figure 3D (AOL-4) depicts a sample in which only a small area of the grain is of primary composition (bright in BSEI) and the surrounding darker BSEI areas have experienced primary alteration.
3. Unaltered grains with penetrating, fracture-controlled secondary alteration grading into highly altered regions which display a conchoidal “hydration front” with low average Z (e.g. LACP-08, Fig. 3E). Conchoidal regions represent metamictized pyrochlore material which has essentially been transformed to glass, has undergone shrinkage during metamictization and destruction of the crystalline structure, followed by late-stage hydration by meteoric and/or hydrothermal fluids. Post-metamictization alteration may be considered a 4th type of alteration in addition to those listed by Lumpkin & Ewing (1995).
4. Heavily altered grains with an intense network or mosaic of fracture-controlled, secondary alteration (e.g. LACP-41, Fig. 3F).
5. Heavily altered grains with crystallographically-controlled (cubic) secondary alteration (e.g. LACP-32B, Fig. 3G). Alteration is controlled by the {111} cleavage of the pyrochlore structure and is reminiscent of exsolution observed in Fe-Ti-oxide phases.

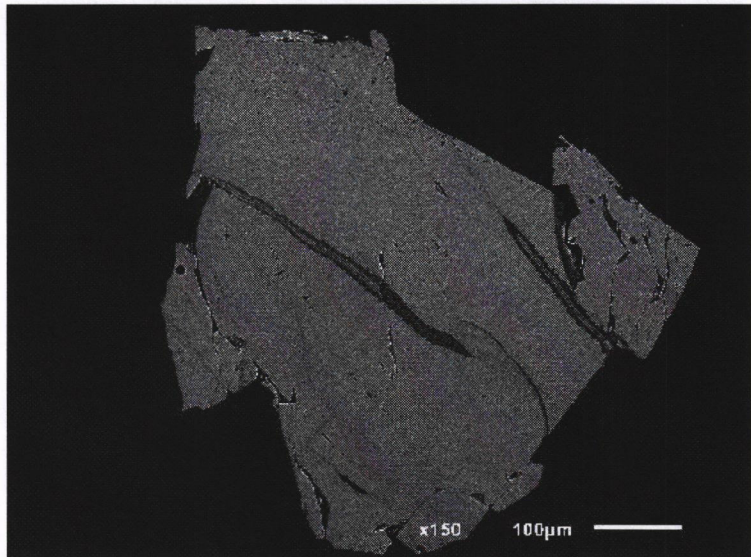


Fig. 3A. Fracture-controlled secondary alteration (LACP-23).

Torstein

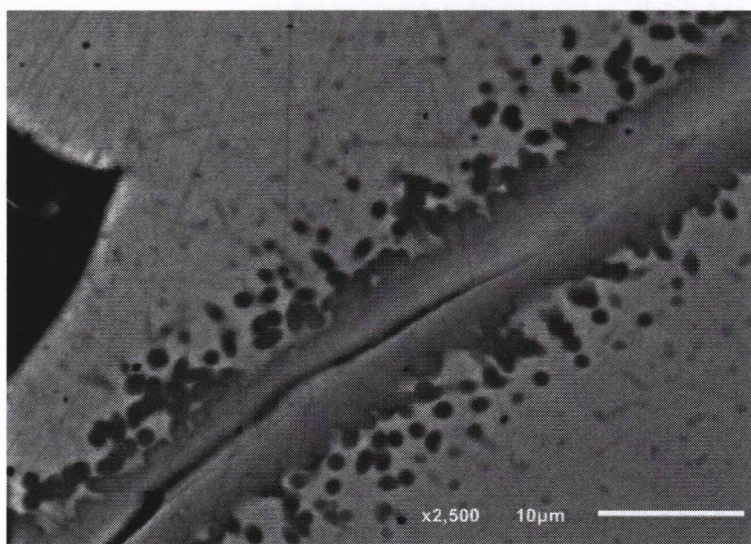


Fig. 3B. Alpha recoil damage in pyrochlore (LACP-23).

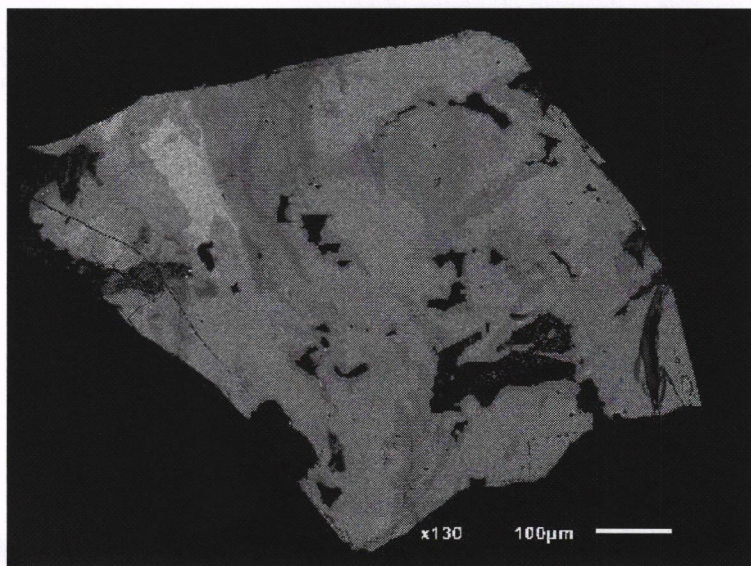


Fig. 3C. Primary and secondary alteration (LACP-01).

Almeningen

Fig. 3D. Primary and secondary alteration (AOL-4).

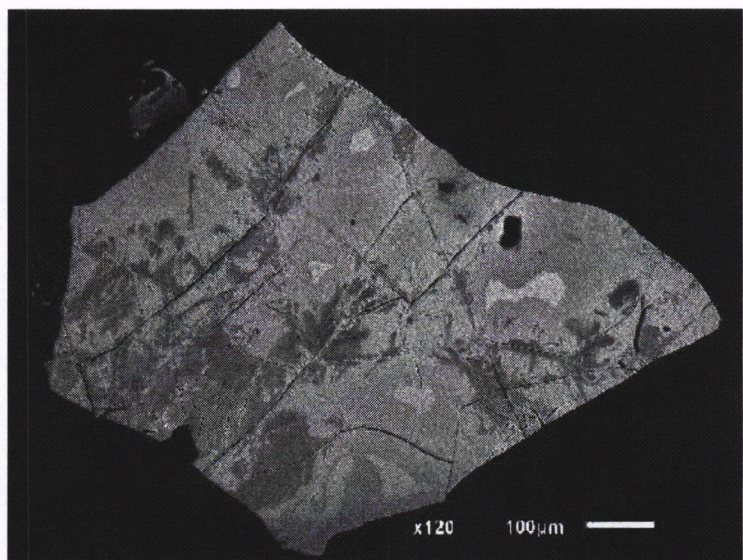


Fig. 3E. Secondary and post-metamictization alteration and hydration (LACP-08). *Tuften*

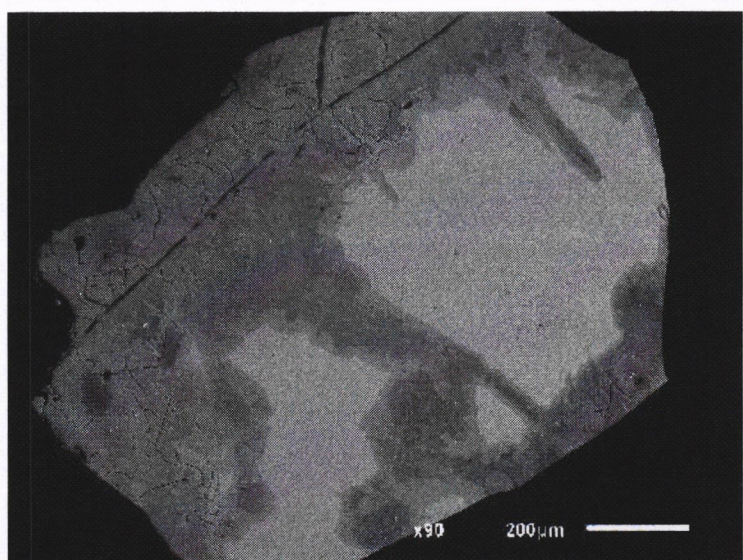
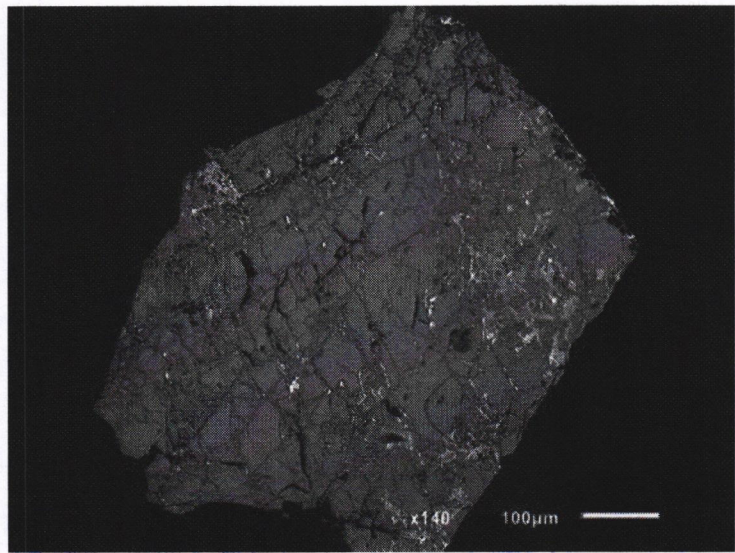


Fig. 3F. Extensive secondary alteration (mosaic; LACP-41).



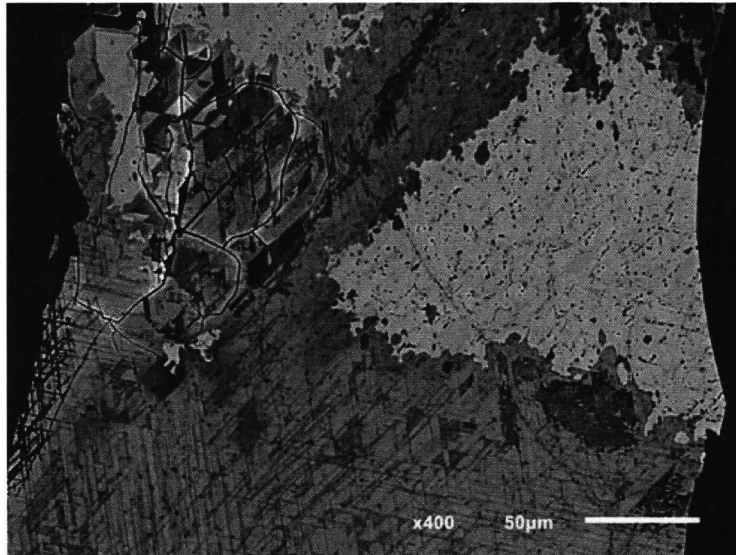


Fig. 3G. Secondary alteration and exsolution (LACP-32B).

Chemical composition

All pyrochlore supergroup minerals analysed from the alkaline pegmatites within the Larvik Plutonic Complex are members of the pyrochlore group *sensu stricto* ($\text{Nb}+\text{Ta}>>2\text{Ti}$ with $\text{Nb}>\text{Ta}$; (Fig. 4).

B-site chemistry

Unaltered pyrochlore from all pegmatite types are Nb-dominant (1.17 – 1.71 apfu, average: 1.47 apfu) with only a minor microlite component ($\text{Ta} = 0.01 – 0.15$ apfu). Titanium contents are variable and range from 0.17 to 0.59 apfu (average: 0.38 apfu), with higher contents generally observed in pyrochlore from miaskitic pegmatites (S- and ST-type; Fig. 5). Other B-site cations include Fe^{3+} (up to 0.10 apfu in pyrochlore from S- and ST8-type pegmatites) and W. Tungsten contents are, on average, negligible (up to 0.03 apfu), with the exception of LACP-01 from the Almenningen quarry (Tvedalen, Larvik; Fig. 3C) where primary compositions are enriched in W (the elsmoreite-group component), with contents up to 0.15 apfu.

Altered pyrochlore display very little deviation in B-site chemistry, similar to their unaltered equivalents. All altered pyrochlore-group minerals are Nb-dominant (0.68 – 1.65 apfu, average: 1.35 apfu), with low Ta contents (range: 0.01 – 0.15 apfu) and Ti contents identical to those observed in unaltered pyrochlore (range: 0.19 – 0.58 apfu; average: 0.37 apfu). Tungsten contents in the altered regions of LACP-01 are similar to those in unaltered regions (up to 0.13 apfu).

Silicon was included in calculation of the Larvik pyrochlore formulae, but interpretations of results are used cautiously – at best, it is suggested that 50% of the Si resides within the pyrochlore structure, whereas 50% resides in amorphous, short-ordered regions, the result of metamictization. Silicon is not present within unaltered pyrochlore, but was detected in high concentrations (up to 0.82 apfu) in grains which have undergone late-stage, post-metamictization hydration of amorphous, glass-like sectors (very dark regions on BSEI).

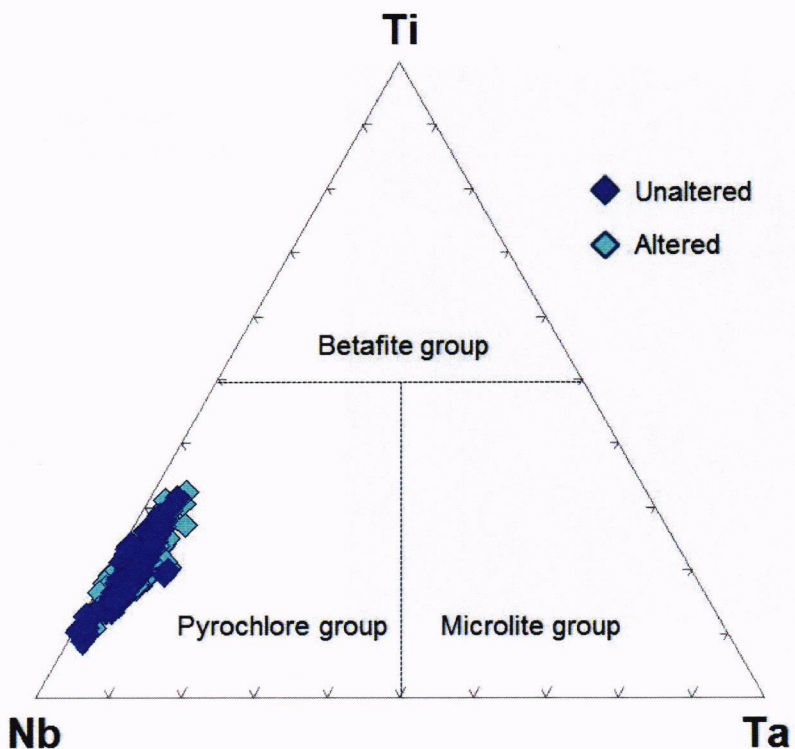


Fig. 4. Unaltered and altered pyrochlore supergroup minerals in the Ti-Nb-Ta ternary diagram. All compositions plot in the pyrochlore-group field.

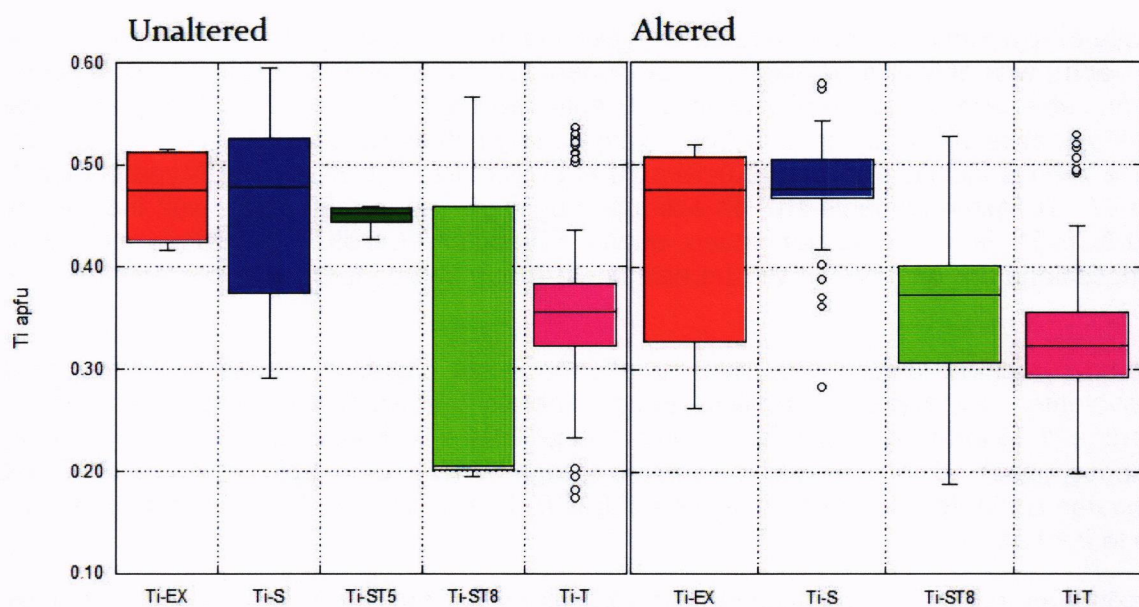


Fig. 5. Range and mean of Ti (apfu) in the *B*-site in unaltered and altered pyrochlore.

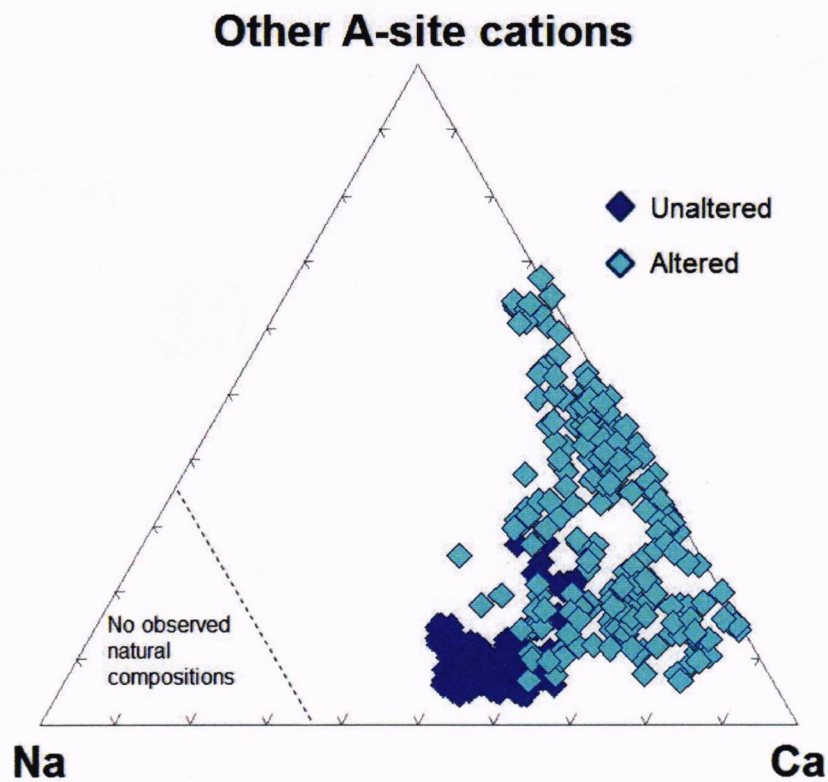


Fig. 6. Composition of unaltered and altered pyrochlore-group minerals in the A-site ternary diagram (Atencio et al., 2010).

A-site chemistry

All unaltered Larvik pyrochlore are Ca-dominant (range: 0.88 to 1.31 apfu, average: 1.07 apfu) with Na contents ranging from 0.33 to 0.86 apfu (average: 0.68 apfu) and can therefore be named as fluorcalciopyrochlore (if $F > 0.50$ apfu) or calciopyrochlore (if $F < 0.50$ apfu; Fig. 6). Average Na contents increase with increasing alkalinity of the pegmatite with the lowest contents found in pegmatites external to the complex ($Na_{ave} = 0.44$ apfu), those within miaskitic pegmatites with moderate values ($Na_{ave} = 0.52 - 0.58$ apfu), and the highest contents found in pyrochlore from T-type mildly agpaitic pegmatites ($Na_{ave} = 0.74$ apfu; Figure 7). The sum of other cations in the A-site (i.e. U, Th, REE, Sr, Pb, Mn, Mg, Y) ranges from 0.09 to 0.51 apfu, with the Σ REE up to 0.19 apfu in samples from miaskitic pegmatites, decreasing to an average of 0.06 apfu in pyrochlore from T-type pegmatites. Both Th (average: 0.03 apfu) and U (average: 0.06 apfu) are minor elements in the A-site. When zoning is observed in BSEI, brighter areas are generally enriched in U (up to 0.15 apfu). Thorium contents are the highest in pyrochlore from pegmatites in the Vardeåsen and Maledøen quarries in RS8 (ST-type; up to 0.14 apfu). Vacancies in the A-site reach a maximum of 15%, with an average of 3%. Vacancies are positively-correlated with Σ REE and decrease from 8% (EX-type) to 4-5% in pyrochlore from miaskitic pegmatites, to only 2% in Na-rich pyrochlore from T-type pegmatites.

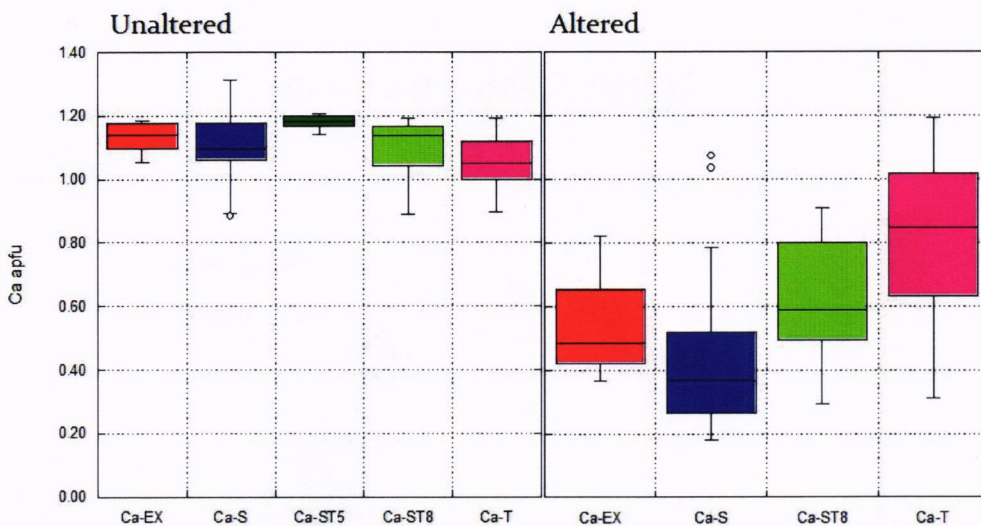


Fig. 7. Range and mean of Na (apfu) in the A-site in unaltered and altered pyrochlore.

Altered pyrochlore-group minerals exhibit a much wider variation in A-site composition than their unaltered counterparts. Calcium contents range from 0.18 to 1.19 apfu (average: 0.70 apfu) and Na contents range from zero to 0.58 apfu (average: 0.14 apfu). Unlike unaltered samples, Ca contents are highest in pyrochlore from T-type pegmatites (average: 0.85 apfu) and decrease in samples from miaskitic pegmatites (0.43 – 0.63 apfu; Figure 8). The sum of other A-site cations ranges from 0.09 to 0.65 apfu (average: 0.32 apfu), slightly higher than observed in unaltered samples. Additional A-site cations in altered samples not observed in unaltered pyrochlore include Sr (max: 0.08 apfu), Mn (max: 0.19 apfu) and K (max: 0.04 apfu). Deficiencies in the A-site are larger than observed in unaltered samples (Figure 9), although it is not possible to determine unequivocally whether these deficiencies are due to vacancies or H₂O. The term “vacancy” is used to encapsulate both possibilities. Vacancies in the A-site range from 10% to 75% (average: 42%), resulting in compositions ranging from calciopyrochlore to kenopyrochlore or hydropyrochlore. As with unaltered samples, pyrochlore in T-type pegmatites, as well as those from ring section 8 (ST8), have the lowest average vacancy content (38% and 34%, respectively) and remain Ca-dominant (calciopyrochlore), unlike those from miaskitic pegmatites which are vacancy-dominant (average: 58% vacancy).

Y-site chemistry

With the exception of LACP-32B from the Klåstad quarry (Tjølling, Larvik; F = 0.38 – 0.43 apfu) and AOL-6 from the Vardeåsen quarry (Pauler, Larvik; F = 0.35 – 0.47 apfu), unaltered samples are F-dominant at the Y site (range: 0.52 – 0.91 apfu). Such species can be described as fluorcalciopyrochlore. Altered samples show more variable F contents (0 – 0.84 apfu, average: 0.32 apfu; Fig. 10). The difficulty in assigning a species name to an analysis occurs when F is not dominant at Y, and A site totals are < 2.00 apfu. Without the benefit of a single crystal X-ray structure refinement, it is impossible to determine the anionic composition of the anion site, Y, and to distinguish between the presence of O, vacancies or H₂O within the A site. An increase in F content is observed with increased alkalinity from S- and ST-type pegmatites to T-type pegmatites.

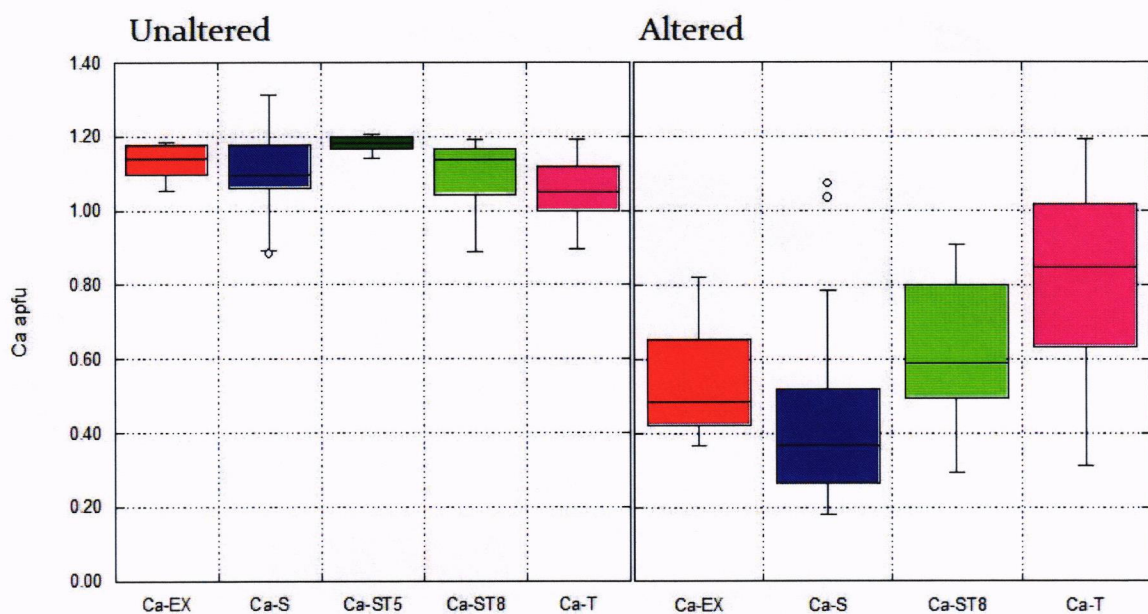


Fig. 8. Range and mean of Ca (apfu) in the A-site in unaltered and altered pyrochlore.

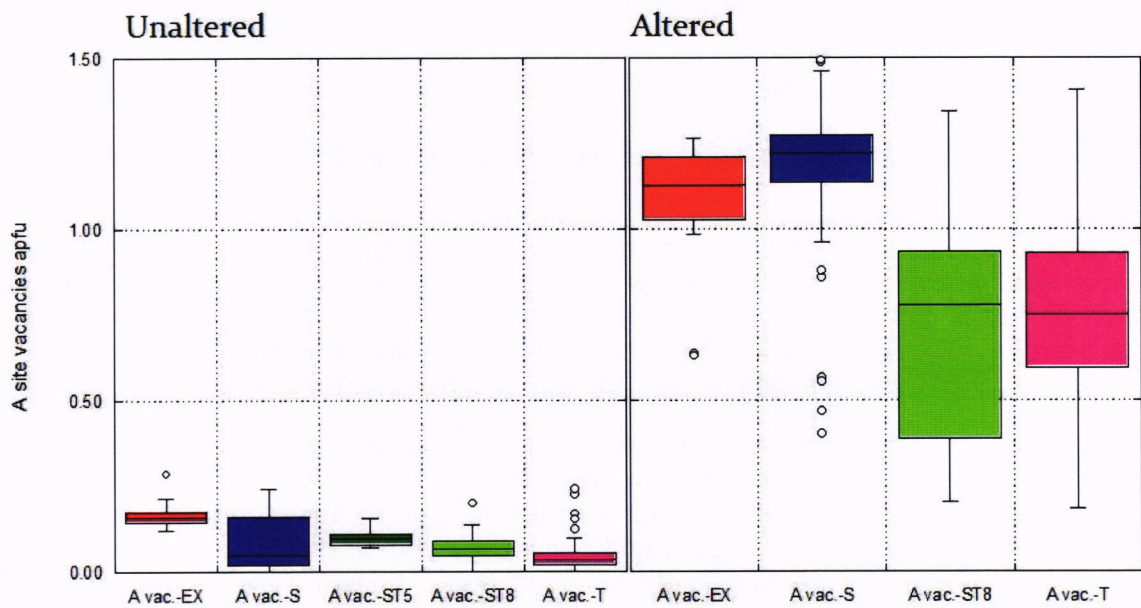


Fig. 9. Range and mean of vacancies (apfu) in the A-site in unaltered and altered pyrochlore.

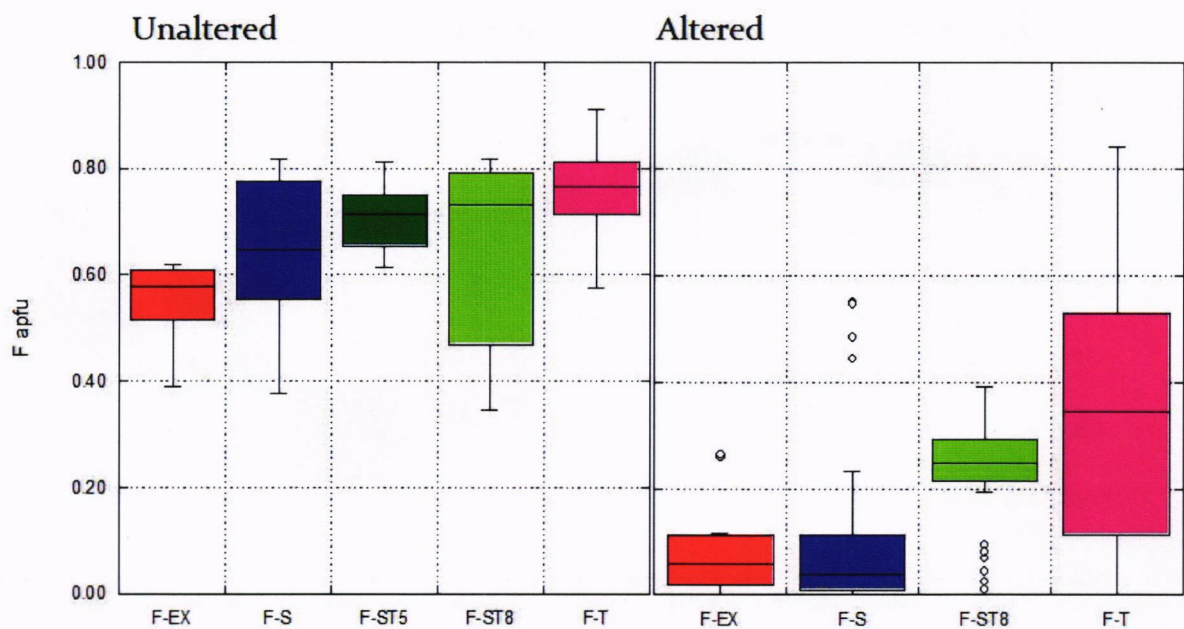


Fig. 10. Range and mean of F (apfu) in the Y-site in unaltered and altered pyrochlore.

Chemical effects of alteration

Alteration of Larvik complex pyrochlore-group minerals can be defined as a three-step process:

1. Primary alteration by high-temperature ($> 150^{\circ}\text{C}$) hydrothermal (post-magmatic) fluids. This stage of alteration results in overprinting of any primary growth features within the pyrochlore and is characterized by moderate replacement of Na and Ca from the A-site by vacancies (Fig. AB), and minor Mn, Fe and Sr, as well as replacement of F by O or OH. (Fig. 11A). B-site cations are immobile and Nb, Ta and Ti contents are not affected by alteration.
2. Secondary alteration by low-temperature ($< 150^{\circ}\text{C}$) meteoric fluids. Secondary alteration is fracture-controlled and is observed in all pyrochlore samples. Alteration around the fractures appears darker on BSEI, and is characterized by near complete loss of Na, extensive loss of Ca with replacement, and dominance, by vacancies in addition to Mn, Fe and Sr. Fluorine is almost completely removed (Fig. 10) and samples are extensively hydrated, as evidenced by the watermark alteration pattern observed around fractures (Fig. 11B). Fig. 12 shows the effects of alteration on the A-site cations in the ternary diagram including the REE. Pyrochlore from miaskitic pegmatites undergo more extensive removal of Ca (and Na) as compared to those from T-type pegmatites, with a concomitant increase in the fraction of REEs.

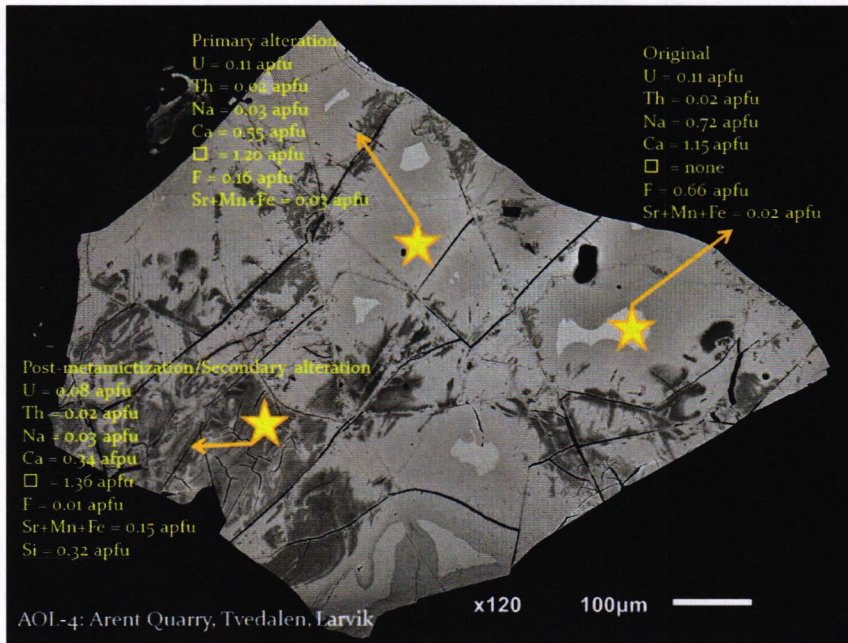


Fig. 11A. Variation in composition between unaltered pyrochlore and regions which have undergone primary, secondary or post-metamictization alteration and hydration. Note the presence of Si only in regions which have undergone extensive alteration and hydration of the metamict, amorphous glass (AOL-4).

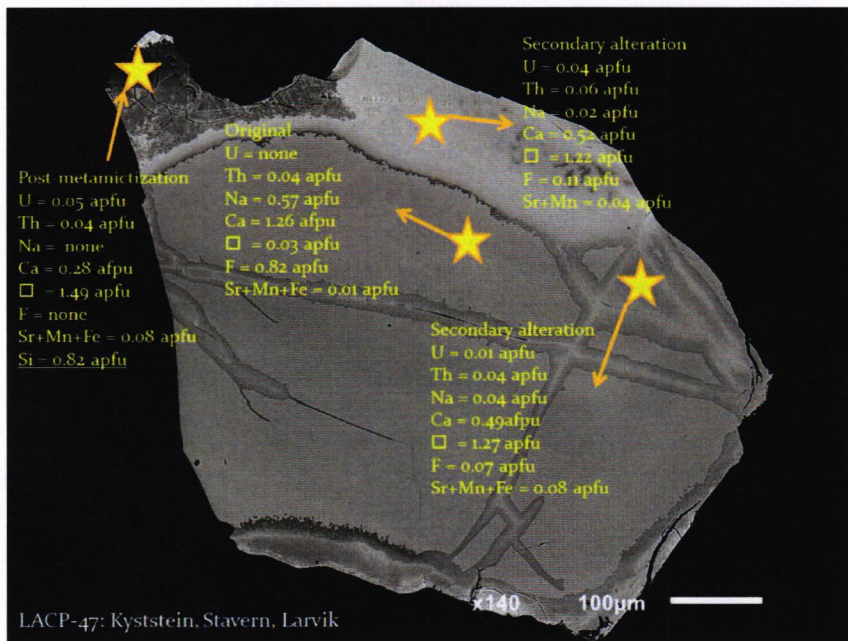


Fig. 11B. Variation in composition between unaltered pyrochlore and regions which have undergone secondary or post-metamictization alteration and hydration. Note the presence of Si only in regions which have undergone extensive alteration and hydration of the metamict, amorphous glass (LACP-47).

3. Post-metamictization hydration occurs during latter stages of secondary alteration. Following destruction of the long-range pyrochlore crystal-structure by alpha radiation, the mineral becomes metamict and amorphous – or glass-like. Hydration of this glass by meteoric fluids, evidenced by the conchoidal, very dark regions on the BSEI (Fig. 11C), results in further removal of cations from the A-site (Ca) and almost complete dominance by vacancies and/or H₂O at both the A- and Y-sites. It is within these highly hydrated regions where upwards of 0.82 apfu of Si is located, further suggesting that Si is present not within a true pyrochlore structure, but held in highly metamict regions dominated by short-range order.

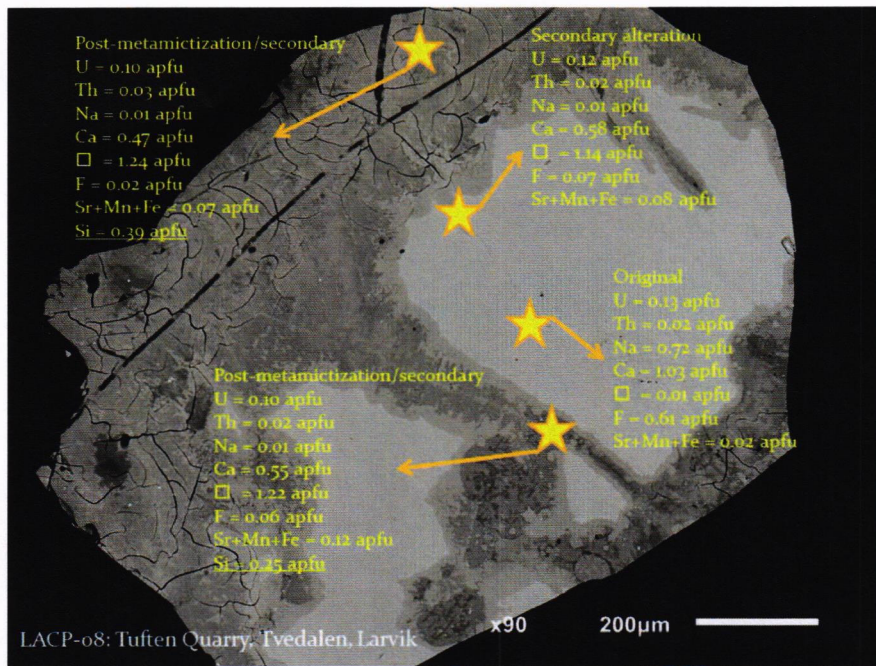


Fig. 11C. Variation in composition between unaltered pyrochlore and regions which have undergone secondary or post-metamictization alteration and hydration. Note the presence of Si only in regions which have undergone extensive alteration and hydration of the metamict, amorphous glass (LACP-08).

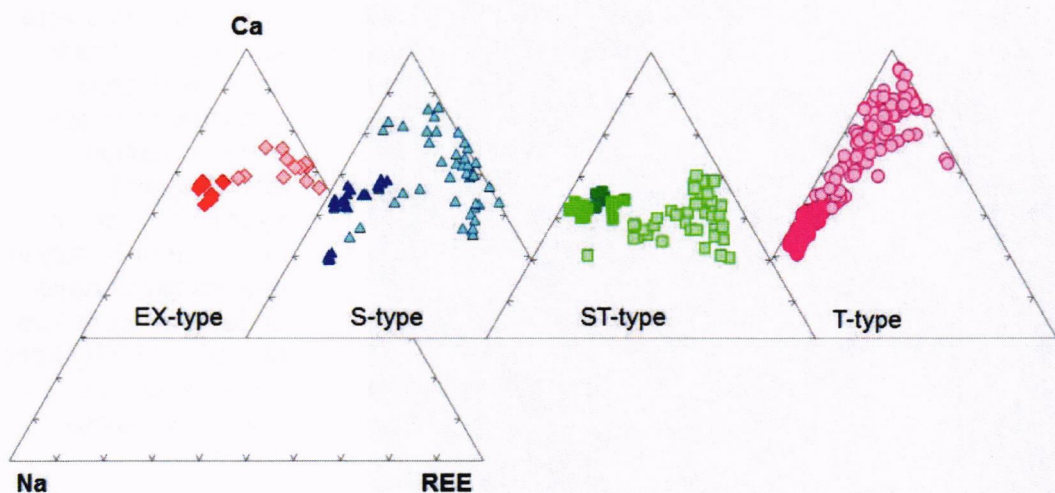


Fig. 12. Ca-Na-REE ternary diagram depicting unaltered (solid fill) and altered (light fill) pyrochlore from EX-, S-, ST- and T-type pegmatites.

Acknowledgements

The authors wish to thank Sven Dahlgren for funding and help with collecting samples in 2004. Thanks also to Andy McDonald for being a field partner, and to Scott Ercit for sharing his extensive knowledge about the pyrochlore supergroup.

References

- ATENCIO, D., ANDRADE, M.B., CHRISTY, A.G., GIERÉ, R. & KARTASHOV, P.M. (2010): The pyrochlore supergroup of minerals: nomenclature. *The Canadian Mineralogist* **48**, 673-698.
- BONAZZI, P., BINDI, L., ZOPPI, M., CAPITANI, G.C. AND OLMI, F. (2006): Single-crystal diffraction and transmission electron microscopy studies of "silicified" pyrochlore from Narssârssuk, Julianehaab district, Greenland. *American Mineralogist* **91**, 794-801.
- CHAKHMOURADIAN, A.R. & MITCHELL, R.H. (2002): New data on pyrochlore- and perovskite-group minerals from the Lovozero alkaline complex, Russia. *European Journal of Mineralogy* **14**, 821-836.
- EDGE, R.A. & TAYLOR, H.F.W. (1971): Crystal structure of thaumasite, $[\text{Ca}_3\text{Si}(\text{OH})_6 \cdot 12\text{H}_2\text{O}](\text{SO}_4)(\text{CO}_3)$. *Acta Crystallographica* **B27**, 594-601.
- FINGER, L.W. & HAZEN, R. (1991): Crystal chemistry of six-coordinated silicon: A key to understanding the earth's deep interior. *Acta Crystallographica*, **47**, 561-580.
- HOGARTH, D.D. (1977): Classification and nomenclature of the pyrochlore group. *American Mineralogist* **62**, 403-410.
- JOHAN, V. & JOHAN, Z. (1994): Accessory minerals of the Cíovec (Zinnwald) granite cupola, Czech Republic Part 1: Nb-, Ta-, and Ti-bearing oxides. *Mineralogy and Petrology* **51**, 323-343.
- LEE, M.J., LEE, J.I., GARCIA, D., MOUTTE, J., WILLIAMS, T.C., WALL, F. & KIM, Y. (2006): Pyrochlore chemistry from the Sokli phoscorite-carbonatite complex, Finland: Implications for the genesis of phoscorite and carbonatite association. *Geochemical Journal* **40**, 1-13.
- LUMPKIN, G.R. & EWING, R.C. (1995): Geochemical alteration of pyrochlore group minerals: pyrochlore subgroup. *American Mineralogist* **80**, 732-743.
- O'KEEFFE, M. & HYDE, B.G. (1981): The role of non-bonded forces in crystals. In *Structure and Bonding in Crystals* (M. O'Keeffe & Navrotsky, eds.). John Wiley & Sons, New York, N.Y., 227-254.
- UHER, P., ČERNÝ, P., CHAPMAN, R., HATÁR, J. & MIKO, O. (1998): Evolution of Nb, Ta-oxide minerals in the Prašivá granitic pegmatites, Slovakia. II. External hydrothermal Pb, Sb overprint. *The Canadian Mineralogist* **36**, 535-545.

Table 1. Pyrochlore supergroup sample localities.

Sample No.	Locality Name	Pegm. Type	RS	Host rock	Morph.
LACP1	Almenningen quarry, Tvedalen, Larvik	T	6	pegmatites in larvikite	dike
LACP4	Saga Pearl quarry, Tvedalen, Larvik	T	6	pegmatite in larvikite	dike
LACP5A1	Saga Pearl quarry, Tvedalen, Larvik	T	6	pegmatite sweats in larvikite	sweats
LACP5A2	Saga Pearl quarry, Tvedalen, Larvik	T	6	pegmatite sweats in larvikite	sweats
LACP6	Tuftan quarry, Tvedalen, Larvik	T	6	old pegmatite in larvikite	dike
LACP7	Tuftan quarry, Tvedalen, Larvik	T	6	pegmatite in larvikite	dike
LACP8	Tuftan quarry, Tvedalen, Larvik	T	6	pegmatites in larvikite	pods
LACP9	Tuftan quarry, Tvedalen, Larvik	T	6	pegmatite in larvikite	dike
LACP10	Tuftan quarry, Tvedalen, Larvik	T	6	pegmatite in larvikite	dike
LACP12	Jahren W, Stavern, Larvik, Vestfold	S	4	pegmatite in larvikite	dike
LACP19	Kariåsen, Vesterøya, Sandefjord	S+	4	altered pegmatite	dike
LACP23	Torstein, Larvik	S	6	pegmatite blocks	dike/pod
LACP30	Saga I quarry, Tvedalen, Larvik, Vestfold	T	6	zoned pegmatite in larvikite	dike
LACP32B	Klåstad quarry, Tjølling, Larvik	S	4	pegmatites in larvikite	dike
LACP39B	Vardåsen quarry, Larvik	ST	8	pegmatite in larvikite	dike
LACP40	Malerød quarry, Larvik	ST	8	pegmatite in larvikite	dike
LACP41A	Gusfred I, Bjørkedalen, Eidanger, Porsgrunn	EX	0	pegmatite in basalt	dike
LACP41B	Gusfred I, Bjørkedalen, Eidanger, Porsgrunn	EX	0	pegmatite in basalt	dike
LACP45	Kuøya (Fuglevik), Stavern, Brunlanes, Larvik	S	4	pegmatite in larvikite	dike & pod
LACP47	Kyststien, Stavern, Larvik	S	4	pegmatite in larvikite	dike
AOL-1	Saga Pearl quarry, Tvedalen, Larvik	T	6	pegmatite in larvikite	dike
AOL-2	Tuftan quarry, Tvedalen, Larvik	T	6	pegmatite in larvikite	dike
AOL-3	Almenningen quarry, Tvedalen, Larvik	T	6	pegmatites in larvikite	dike
AOL-4	Arent quarry, Tvedalen, Larvik	T	6	pegmatite in larvikite	dike
AOL-5	Håkestad quarry, Tjølling, Larvik	ST	5	pegmatites in larvikite	dike/pod
AOL-6	Vardåsen quarry, Larvik	ST	8	pegmatite in larvikite	dike

Pegm. Type: Pegmatite Type. T = Tvedalen type, S = Stavern type, ST = Stålaker type, EX = external type.

RS: Ring Section

Morph.: Dike Morphology

Table 2. Representative EMP analyses of LPC pyrochlores.

Wt.%	Unaltered EX-type pegmatites			Altered EX-type pegmatites			Unaltered S-type pegmatites		
	Average	Min	Max	Average	Min	Max	Average	Min	Max
Na ₂ O	3,59	2,64	4,00	0,50	0,04	1,80	4,66	2,61	6,21
K ₂ O	0,00	0,00	0,02	0,06	0,04	0,10	0,01	0,00	0,03
CaO	16,89	15,51	17,94	8,69	5,87	12,43	15,76	12,65	19,57
SrO	0,27	0,06	0,59	0,74	0,46	1,22	0,01	0,00	0,08
PbO	0,13	0,07	0,23	0,10	0,03	0,17	0,19	0,01	0,42
MgO	0,00	0,00	0,00	0,00	0,00	0,01	0,00	0,00	0,01
MnO	0,32	0,14	0,79	0,71	0,49	0,88	0,18	0,00	0,62
Fe ₂ O ₃	0,26	0,15	0,41	0,69	0,37	2,02	0,88	0,12	4,83
Al ₂ O ₃	0,00	0,00	0,01	0,03	0,00	0,12	0,03	0,00	0,08
Y ₂ O ₃	0,40	0,28	0,51	0,89	0,46	2,34	0,32	0,04	0,83
La ₂ O ₃	1,39	1,21	1,57	1,49	1,25	1,75	0,90	0,35	1,45
Ce ₂ O ₃	4,23	3,20	5,26	4,93	4,00	5,47	2,72	1,18	4,30
Nd ₂ O ₃	0,85	0,53	1,15	1,19	0,78	1,61	0,78	0,24	1,19
Sm ₂ O ₃	0,08	0,00	0,17	0,18	0,10	0,34	0,10	0,00	0,21
Pr ₂ O ₃	0,00	0,00	0,00	0,00	0,00	0,00	0,23	0,08	0,43
SiO ₂	0,01	0,00	0,04	1,77	0,05	5,61	0,01	0,00	0,25
TiO ₂	9,96	8,96	10,79	9,82	6,34	11,35	9,24	6,21	12,00
ZrO ₂	0,71	0,48	0,89	0,70	0,22	1,19	1,18	0,29	2,13
HfO ₂	0,03	0,00	0,07	0,01	0,00	0,04	0,01	0,00	0,10
SnO ₂	0,09	0,03	0,13	0,09	0,04	0,12	0,08	0,00	0,28
ThO ₂	3,90	3,06	4,46	4,51	3,02	6,53	3,15	1,01	6,63
UO ₂	0,65	0,03	1,38	0,92	0,03	1,47	5,08	0,32	10,30
Nb ₂ O ₅	51,41	48,50	55,09	51,77	49,28	60,36	48,08	42,18	57,16
Ta ₂ O ₅	1,90	0,99	2,60	2,06	0,54	2,77	3,50	2,44	4,73
SO ₃	0,02	0,00	0,07	0,02	0,00	0,07	0,02	0,00	0,06
WO ₃	0,29	0,06	0,66	0,25	0,07	0,65	0,24	0,04	0,70
F	2,77	1,94	3,18	0,45	0,00	1,36	3,08	1,84	4,19
O=F	-1,17	-1,34	-0,82	-0,19	-0,57	0,00	-1,30	-1,76	-0,77
TOTAL	98,97	97,74	100,10	92,37	89,95	95,83	99,03	97,27	100,29

Formulae based on 1 B-site cation									
Na	0,44	0,33	0,49	0,06	0,01	0,21	0,58	0,33	0,79
K	0,00	0,00	0,00	0,00	0,00	0,01	0,00	0,00	0,00
Ca	1,13	1,05	1,18	0,55	0,37	0,82	1,09	0,88	1,31
Sr	0,01	0,00	0,02	0,03	0,02	0,04	0,00	0,00	0,00
Pb	0,00	0,00	0,00	0,00	0,00	0,00	0,00	0,00	0,01
Mg	0,00	0,00	0,00	0,00	0,00	0,00	0,00	0,00	0,00
Mn	0,02	0,01	0,04	0,04	0,02	0,05	0,01	0,00	0,03
Y	0,01	0,01	0,02	0,03	0,02	0,07	0,01	0,00	0,03
La	0,03	0,03	0,04	0,03	0,03	0,04	0,02	0,01	0,04
Ce	0,10	0,07	0,12	0,11	0,08	0,12	0,06	0,03	0,10
Nd	0,02	0,01	0,03	0,02	0,02	0,03	0,02	0,01	0,03
Sm	0,00	0,00	0,00	0,00	0,00	0,01	0,00	0,00	0,01
Th	0,06	0,04	0,07	0,06	0,04	0,08	0,05	0,02	0,10
U	0,01	0,00	0,02	0,01	0,00	0,02	0,07	0,00	0,15
S	0,00	0,00	0,00	0,00	0,00	0,00	0,00	0,00	0,00
SA	1,83	1,71	1,88	0,94	0,73	1,37	1,92	1,76	2,02
A vac.	0,17	0,12	0,29	1,06	0,63	1,27	0,08	0,00	0,24
Fe ³⁺	0,01	0,01	0,02	0,03	0,02	0,08	0,04	0,01	0,22
Al	0,00	0,00	0,00	0,00	0,00	0,01	0,00	0,00	0,01
Si	0,00	0,00	0,00	0,10	0,00	0,31	0,00	0,00	0,02
Ti	0,47	0,42	0,52	0,44	0,26	0,52	0,45	0,29	0,59
Zr	0,02	0,01	0,03	0,02	0,01	0,03	0,04	0,01	0,07
Hf	0,00	0,00	0,00	0,00	0,00	0,00	0,00	0,00	0,00
Sn	0,00	0,00	0,00	0,00	0,00	0,00	0,00	0,00	0,01
Nb	1,46	1,39	1,53	1,37	1,30	1,55	1,40	1,25	1,59
Ta	0,03	0,02	0,05	0,03	0,01	0,05	0,06	0,04	0,09
W	0,00	0,00	0,01	0,00	0,00	0,01	0,00	0,00	0,01
SB	2,00	2,00	2,00	2,00	2,00	2,00	2,00	2,00	2,00
F	0,55	0,39	0,62	0,09	0,00	0,26	0,63	0,38	0,82
OH/H ₂ O	0,45	0,38	0,61	0,91	0,74	1,00	0,37	0,18	0,62
SY	1,00	1,00	1,00	1,00	1,00	1,00	1,00	1,00	1,00
O	6,23	6,18	6,28	5,73	5,49	6,03	6,23	5,96	6,43

Table 2. Cont.

Wt.%	Altered S-type pegmatites			Unaltered ST5-type pegmatites			Unaltered ST8-type pegmatites		
	Average	Min	Max	Average	Min	Max	Average	min	max
Na ₂ O	0,50	0,02	4,23	4,36	4,09	4,71	4,84	3,08	5,60
K ₂ O	0,10	0,01	0,42	0,01	0,00	0,02	0,01	0,00	0,63
CaO	6,55	3,10	14,95	17,87	17,43	18,46	16,48	13,71	17,63
SrO	0,46	0,00	1,13	0,02	0,00	0,11	0,01	0,00	1,36
PbO	0,24	0,03	0,75	0,10	0,06	0,15	0,10	0,00	0,34
MgO	0,02	0,00	0,19	0,00	0,00	0,01	0,00	0,00	0,09
MnO	0,85	0,05	1,69	0,52	0,45	0,60	0,28	0,08	1,32
Fe ₂ O ₃	1,18	0,18	2,66	0,52	0,36	0,83	1,14	0,66	11,96
Al ₂ O ₃	0,09	0,00	1,39	0,01	0,00	0,03	0,06	0,04	0,50
Y ₂ O ₃	0,55	0,00	1,37	0,34	0,26	0,41	0,41	0,20	2,21
La ₂ O ₃	1,13	0,37	1,50	1,20	0,97	1,42	0,87	0,49	3,12
Ce ₂ O ₃	3,45	1,16	5,38	3,53	2,88	3,99	2,15	1,08	8,79
Nd ₂ O ₃	0,97	0,17	1,96	0,53	0,40	0,64	0,44	0,15	2,41
Sm ₂ O ₃	0,11	0,00	0,20	0,05	0,00	0,15	0,06	0,00	0,37
Pr ₂ O ₃	0,26	0,06	0,72	0,20	0,12	0,29	0,29	0,21	0,48
SiO ₂	1,82	0,00	17,48	0,02	0,00	0,11	0,04	0,00	13,04
TiO ₂	10,47	7,21	13,13	9,71	9,33	9,92	5,59	4,03	10,80
ZrO ₂	1,12	0,35	2,53	1,30	0,93	1,85	2,07	1,76	23,47
HfO ₂	0,01	0,00	0,07	0,00	0,00	0,02	0,07	0,00	0,64
SnO ₂	0,09	0,00	0,41	0,21	0,11	0,32	0,52	0,03	0,84
ThO ₂	4,15	1,05	7,98	2,05	1,81	2,36	4,75	2,60	9,04
UO ₂	6,35	0,53	12,10	0,05	0,00	0,07	1,09	0,03	6,44
Nb ₂ O ₅	46,45	31,82	56,68	51,86	50,98	52,76	53,26	40,01	58,50
Ta ₂ O ₅	3,72	2,37	6,18	1,22	0,88	1,42	1,88	0,69	3,97
SO ₃	0,02	0,00	0,07	0,01	0,00	0,04	0,01	0,00	0,10
WO ₃	0,21	0,02	0,63	0,87	0,69	1,07	0,70	0,14	0,84
F	0,50	0,00	2,60	3,61	3,19	4,13	3,46	1,91	4,08
O=F	-0,21	-1,09	0,00	-1,52	-1,74	-1,34	-1,46	-1,76	0,00
TOTAL	90,98	84,43	97,27	98,65	98,05	99,60	98,97	97,01	100,12

Formulae based on 1 B-site cation

Na	0,06	0,00	0,52	0,52	0,48	0,56	0,60	0,41	0,67
K	0,01	0,00	0,03	0,00	0,00	0,00	0,00	0,00	0,04
Ca	0,43	0,18	1,07	1,18	1,14	1,21	1,13	1,02	1,17
Sr	0,02	0,00	0,04	0,00	0,00	0,00	0,00	0,00	0,04
Pb	0,00	0,00	0,01	0,00	0,00	0,00	0,00	0,00	0,01
Mg	0,00	0,00	0,02	0,00	0,00	0,00	0,00	0,00	0,01
Mn	0,04	0,00	0,09	0,03	0,02	0,03	0,02	0,00	0,06
Y	0,02	0,00	0,04	0,01	0,01	0,01	0,01	0,01	0,06
La	0,03	0,01	0,03	0,03	0,02	0,03	0,02	0,01	0,08
Ce	0,08	0,03	0,11	0,08	0,07	0,09	0,05	0,02	0,23
Nd	0,02	0,00	0,04	0,01	0,01	0,01	0,01	0,00	0,06
Sm	0,00	0,00	0,00	0,00	0,00	0,00	0,00	0,00	0,01
Th	0,06	0,01	0,10	0,03	0,03	0,03	0,07	0,04	0,14
U	0,09	0,01	0,18	0,00	0,00	0,00	0,02	0,00	0,10
S	0,00	0,00	0,00	0,00	0,00	0,00	0,00	0,00	0,01
SA	0,85	0,51	1,60	1,90	1,84	1,93	1,94	1,86	1,96
A vac.	1,15	0,40	1,49	0,10	0,07	0,16	0,06	0,00	1,35
Fe ³⁺	0,05	0,01	0,12	0,02	0,02	0,04	0,06	0,03	0,46
Al	0,01	0,00	0,08	0,00	0,00	0,00	0,01	0,00	0,03
Si	0,10	0,00	0,82	0,00	0,00	0,01	0,00	0,00	0,67
Ti	0,47	0,28	0,58	0,45	0,43	0,46	0,27	0,19	0,57
Zr	0,03	0,01	0,07	0,04	0,03	0,06	0,06	0,06	0,59
Hf	0,00	0,00	0,00	0,00	0,00	0,00	0,00	0,00	0,01
Sn	0,00	0,00	0,01	0,01	0,00	0,01	0,01	0,00	0,02
Nb	1,27	0,68	1,50	1,44	1,42	1,46	1,54	1,25	1,64
Ta	0,06	0,04	0,11	0,02	0,02	0,02	0,03	0,01	0,08
W	0,00	0,00	0,01	0,01	0,01	0,02	0,01	0,00	0,01
SB	2,00	2,00	2,00	2,00	2,00	2,00	2,00	2,00	2,00
F	0,10	0,00	0,55	0,70	0,62	0,81	0,70	0,42	0,80
OH/H ₂ O	0,90	0,45	1,00	0,30	0,19	0,39	0,30	0,18	1,00
SY	1,00	1,00	1,00	1,00	1,00	1,00	1,00	1,00	1,00
O	5,62	4,96	6,08	6,16	6,12	6,23	6,21	6,03	6,45

Table 2. Cont.

	Altered ST8-type pegmatites			Unaltered T-type pegmatites			Altered T-type pegmatites		
Wt.%	Average	Min	Max	Average	Min	Max	Average	Min	Max
Na ₂ O	1,19	0,09	3,90	5,97	3,80	6,91	1,41	0,03	4,80
K ₂ O	0,07	0,00	0,63	0,01	0,00	0,05	0,11	0,00	0,39
CaO	8,71	4,12	13,30	15,37	12,70	17,34	12,55	5,36	18,38
SrO	0,16	0,00	1,36	0,02	0,00	0,18	0,44	0,00	2,28
PbO	0,15	0,00	0,34	0,19	0,00	0,39	0,18	0,00	0,73
MgO	0,01	0,00	0,09	0,00	0,00	0,02	0,00	0,00	0,06
MnO	0,75	0,46	1,32	0,05	0,00	0,30	0,56	0,00	3,57
Fe ₂ O ₃	3,51	1,00	11,96	0,29	0,05	1,36	0,63	0,05	2,28
Al ₂ O ₃	0,15	0,06	0,50	0,02	0,00	0,06	0,06	0,00	0,28
Y ₂ O ₃	1,12	0,69	2,21	0,13	0,00	0,48	0,24	0,00	1,67
La ₂ O ₃	2,27	1,29	3,12	0,55	0,21	1,07	0,67	0,19	2,78
Ce ₂ O ₃	6,50	3,54	8,79	1,55	0,55	2,94	1,82	0,52	6,50
Nd ₂ O ₃	1,75	0,56	2,41	0,40	0,11	0,84	0,47	0,06	2,27
Sm ₂ O ₃	0,22	0,06	0,37	0,05	0,00	0,27	0,06	0,00	0,36
Pr ₂ O ₃	0,34	0,20	0,48	0,20	0,00	0,32	0,11	0,05	0,18
SiO ₂	1,62	0,00	13,04	0,01	0,00	0,24	1,57	0,00	8,17
TiO ₂	7,28	4,87	10,80	7,45	3,63	11,16	7,09	4,10	11,16
ZrO ₂	2,90	1,07	23,47	1,18	0,36	1,91	1,23	0,35	1,90
HfO ₂	0,04	0,00	0,64	0,02	0,00	0,09	0,02	0,00	0,09
SnO ₂	0,19	0,06	0,49	0,19	0,00	1,20	0,13	0,00	0,79
ThO ₂	7,05	4,73	9,04	1,72	0,39	3,61	1,98	0,45	4,00
UO ₂	2,93	0,03	6,44	4,71	0,15	8,93	4,90	0,83	9,24
Nb ₂ O ₅	39,81	23,07	49,67	51,51	43,96	59,46	50,02	37,83	58,03
Ta ₂ O ₅	3,32	1,13	3,97	3,99	0,77	8,30	4,11	0,91	8,09
SO ₃	0,03	0,00	0,10	0,02	0,00	0,07	0,03	0,00	0,31
WO ₃	0,16	0,00	0,55	1,54	0,04	8,75	1,11	0,01	7,75
F	1,05	0,00	1,97	3,77	2,78	4,56	1,66	0,00	4,04
O=F	-0,44	-0,83	0,00	-1,59	-1,92	-1,17	-0,70	-1,70	0,00
TOTAL	92,61	87,44	98,56	99,13	97,58	100,44	92,34	83,18	98,25
<i>Formulae based on 1 B-site cation</i>									
Na	0,16	0,01	0,51	0,74	0,48	0,86	0,17	0,00	0,59
K	0,01	0,00	0,04	0,00	0,00	0,00	0,01	0,00	0,03
Ca	0,63	0,29	0,99	1,05	0,90	1,19	0,85	0,31	1,55
Sr	0,01	0,00	0,04	0,00	0,00	0,01	0,02	0,00	0,08
Pb	0,00	0,00	0,01	0,00	0,00	0,01	0,00	0,00	0,01
Mg	0,00	0,00	0,01	0,00	0,00	0,00	0,00	0,00	0,01
Mn	0,04	0,02	0,06	0,00	0,00	0,02	0,03	0,00	0,19
Y	0,04	0,02	0,06	0,00	0,00	0,02	0,01	0,00	0,05
La	0,06	0,03	0,08	0,01	0,01	0,03	0,02	0,00	0,06
Ce	0,16	0,07	0,23	0,04	0,01	0,07	0,04	0,01	0,14
Nd	0,04	0,01	0,06	0,01	0,00	0,02	0,01	0,00	0,05
Sm	0,00	0,00	0,01	0,00	0,00	0,01	0,00	0,00	0,01
Th	0,11	0,06	0,14	0,02	0,01	0,05	0,03	0,01	0,06
U	0,04	0,00	0,10	0,07	0,00	0,13	0,07	0,01	0,13
S	0,00	0,00	0,01	0,00	0,00	0,00	0,00	0,00	0,01
SA	1,30	0,65	1,86	1,96	1,76	2,07	1,25	0,59	2,01
A vac.	0,70	0,14	1,35	0,04	0,00	0,24	0,75	0,00	1,41
Fe ³⁺	0,17	0,04	0,46	0,01	0,00	0,07	0,03	0,00	0,10
Al	0,01	0,00	0,03	0,00	0,00	0,01	0,00	0,00	0,02
Si	0,10	0,00	0,67	0,00	0,00	0,02	0,09	0,00	0,45
Ti	0,36	0,19	0,57	0,36	0,17	0,54	0,33	0,20	0,56
Zr	0,08	0,04	0,59	0,04	0,01	0,06	0,04	0,01	0,06
Hf	0,00	0,00	0,01	0,00	0,00	0,00	0,00	0,00	0,00
Sn	0,01	0,00	0,01	0,00	0,00	0,03	0,00	0,00	0,02
Nb	1,20	0,54	1,39	1,49	1,31	1,71	1,41	1,09	1,65
Ta	0,06	0,02	0,08	0,07	0,01	0,15	0,07	0,02	0,15
W	0,00	0,00	0,01	0,03	0,00	0,15	0,02	0,00	0,13
SB	2,00	2,00	2,00	2,00	2,00	2,00	2,00	2,00	2,00
F	0,23	0,00	0,44	0,76	0,57	0,91	0,33	0,00	0,84
OH/H ₂ O	0,77	0,56	1,00	0,24	0,09	0,43	0,67	0,16	1,00
SY	1,00	1,00	1,00	1,00	1,00	1,00	1,00	1,00	1,00
O	5,97	4,98	6,45	6,13	5,97	6,38	5,87	5,31	6,70